energies

MDPI

Article

Influence of the Selection of the Core Shape and Winding Arrangement on the Accuracy of Current Transformers with Through-Going Primary Cable

Elzbieta Lesniewska

Institute of Mechatronics and Information Systems, Lodz University of Technology, 90-924 Lodz, Poland; elzbieta.lesniewska-komeza@p.lodz.pl; Tel.: +48-42-6312694

Abstract: The current transformers with split-core are used for installation in places where it is impossible to install classic current transformers. Moreover, this design allows for any measurement location change, and even switching one current transformer into several different shapes of bars or cables. Power network operators, striving for more accurate current measurements, require producers to provide current transformers with a special accuracy class 0.2S. Therefore, manufacturers and designers try to meet the market requirements and, similarly to non-demountable current transformers, i.e., with a toroidal core, design current transformers with split-core class 0.2S. To meet the high metrological requirements, 3D analyses of electromagnetic fields were performed, taking into account physical phenomena and not approximate analytical models. Two types of cores and four different arrangements of the secondary windings of the measuring current transformers were considered. The magnetic field distributions, current error, and phase displacement diagrams of all current transformer models were analyzed, and the model of the transformer structure with the best accuracy was selected. Computations were conducted based on the finite element numerical method, and the results were compared with the real model tests.

Keywords: split-core; current transformers accuracy; finite element method

Citation: Lesniewska, E. Influence of the Selection of the Core Shape and Winding Arrangement on the Accuracy of Current Transformers with Through-Going Primary Cable. *Energies* **2021**, *14*, 1932. https://doi.org/10.3390/en14071932

Academic Editor: Sérgio Cruz

Received: 12 February 2021
Accepted: 28 March 2021
Published: 31 March 2021

1. Introduction

The measuring current transformer as part of the measuring system must meet the requirements of the International Electrotechnical Commission and the European Standard (IEC/EN) [1,2]. IEC/EN Current transformer (CT) transformation errors influence measurement errors. Therefore, manufacturers must strive to reduce the errors of the designed current transformer. Through-hole CTs are usually built with the secondary winding evenly distributed over the toroidal core and with a through-line primary conductor. This series of current transformers is designed for distribution systems using cables or busbars. They can be mounted both on the bar and on the wall.

The current error and the phase displacement of the current transformer indicate the accuracy class of the designed current transformer. Table 1 shows the accuracy limits for the different classes of current transformers.

The IEC/EN standards [1,2] define transformation errors as current error:

$$\Delta_i = \frac{I_s K_n - I_p}{I_p} \cdot 100\% \tag{1}$$

and phase displacement

$$\delta_i = \varphi_{i_s} - \varphi_{i_p} \tag{2}$$

where I_p and I_s are the RMS values of the primary and secondary current, φ_{i_p} and φ_{i_s} are the phase angles of these currents, respectively, and K_n is the CT ratio.

Table 1. Standard classes of current transformers according to IEC/EN 61869-2.

Class / (± %) I_{pn}	Current Errors (± %)					Phase Displacement (± min)				
	1	**5**	**20**	**100**	**120**	**1**	**5**	**20**	**100**	**120**
0.1	—	0.2	0.1	0.1	0.1	—	15	8	5	5
0.2S	0.75	0.35	0.2	0.2	0.2	30	15	10	10	10
0.2	—	0.75	0.35	0.2	0.2	—	30	15	10	10
0.5S	1.5	0.75	0.5	0.5	0.5	90	45	30	30	30
0.5	—	1.5	0.75	0.5	0.5	—	90	45	30	30

Instrument transformers are precision devices. Class 0.2 means that the current error (1) at the rated value is less than 0.2%, and the phase displacement (2) is measured in minutes; therefore, an error of 10 min means 0.17 degrees. In addition, the standard specifies the permissible values of current and phase displacement at the measured primary current equal to 5%, 20%, 100% and 120% of the rated current. The special class 0.2S additionally determines the accuracy with a very low primary current of 1% of the rated value.

Currently, instead of ordinary class 0.2 class current transformers, the designers of measurement systems, following the requirements set by network operators, provide the installation of current transformers of special 0.2S accuracy classes. This situation is practically common for low voltage toroidal current transformers. The growing metrological requirements for class S current transformers are accompanied by problems with designing their magnetic circuits, which do not occur in the usual accuracy classes.

Split-core current transformers can measure the current without interrupting the electrical supply. They are used in distribution panels or power centers for maintenance or system expansion. They are easy to install, which saves a lot of time by avoiding bar disconnection. Split-core CTs, which can be found in company catalogs, usually have a class of at most 0.5 (and 1 and 3), while more accurate CTs with a higher class of 0.2 and 0.2S are also required.

Split-cores have been used for some time in electromagnetic interference (EMI) suppressors as a sleeve core that encircles the cables. Two split parts manufacture this construction, pressed together by a snap-on mechanism, which turns this into a quick, easy to install solution [3]. Such solutions are also used in the case of wireless sensors in the power system [4,5], transformers [6], and also current transformers [7–9].

In order to meet the high metrological requirements when creating device models, real physical phenomena should be taken into account and not analytical approximate models (equivalent circuits) should be used. Many authors use the 3D finite element method when designing electromagnetic devices, such as motors [10], power transformers [11,12], instrument transformers [13–18], and other types of transducers [19]. This method allows determination of the properties of devices at the design stage, before making a prototype. It gives much more accurate results than analytical methods. Therefore, three-dimensional models of current transformers were used, and problems were solved using the numerical field-circuit method.

A comparator based on a commonly used method was used to measure transformation errors. The measurement is performed with the use of the scheme of a differential circuit for AC compensation of 50 or 60 Hz, using a higher class standard current transformer with the same ratio as the transformer under test. However, in the case of other types of transducers, such as optoelectronic [20] or current-voltage transducers [19], other measurement methods are of course used. Other measurement systems are also required to measure current transformer transformation errors with distorted supply voltages [21,22]. By using these circuits, it is also possible to measure transformation errors when supplying voltages with only a basic harmonic, although it is not necessary.

The purpose of the study was to evaluate in the design process how the transformation errors would change when, instead of a toroidal core, we use a split-core with the same cross-section and magnetization path but with a different secondary winding arrangement.

The accuracy of the applied method has been confirmed by tests performed for the toroidal current transformer.

The rest of this paper is structured as follows.

Section 2 presents the geometric models of the 600 A/5 A current transformer constructions with a through-going primary cable and with the use of a split-core, as well as the magnetization and loss characteristics of the transformer steel used at theses cores.

Section 3 describes the mathematical model and computer simulation data. Section 4 compares the results of the simulation and experimental tests. A comparison of transformation error calculations for various transformer models, their prototypes, and comments on accuracy are presented. Finally, the practical conclusions of the research end this work in Section 5.

2. Construction of CT

The research was carried out on four types of current transformers (600 A/5 A) shown in Figure 1: one with a toroidal core and three with a split-core. Furthermore, it was assumed that all four cores, with the same cross-section (S = 202.5 mm^2) and the same magnetization length (l = 178.3 mm), were made using the same transformer steel. Figure 2 shows the geometric model 3 of a split-core current transformer when mounted on a switchboard without disconnecting the bars. The magnetization characteristics and the specific power loss characteristics of the steel used are shown in Figure 3. However, different secondary winding arrangements with the same number of turns were used in the CTs.

The secondary winding of the 600 A/5 A transformer had 120 turns wound with a Φ1.2 mm wire. The secondary winding was centrally located in the:

- Toroid evenly around the circumference (Figure 1a);
- Model 1, centrally on one column, in 2 layers, 60 turns each (Figure 1b);
- Model 2, centrally on two columns, in one layer, 60 turns (Figure 1c);
- Model 3, centrally on four columns, in one layer, 30 turns each (Figure 1d).

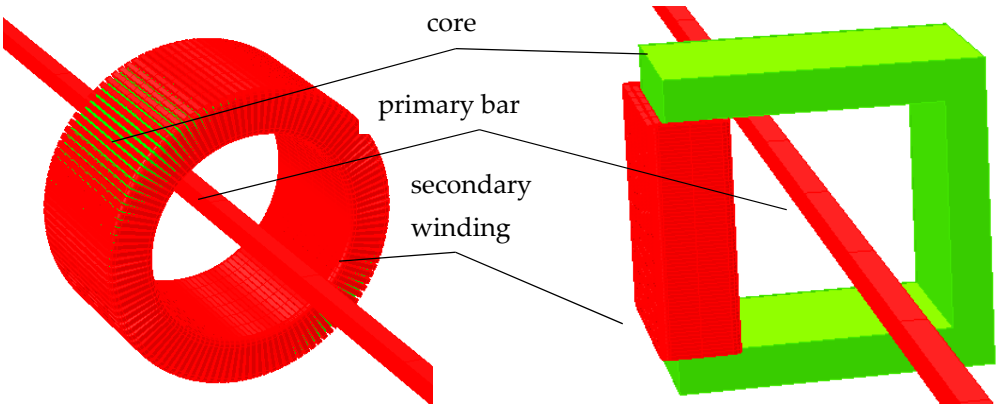

(**a**) toroidal core (dimension: diameters d_1 = 63.5 mm; d_2 = 50 mm, height h = 30 mm).

(**b**) split-core—model 1 (dimension: external a = 51.32 mm; internal b = 37.82 mm, height h = 30 mm).

Figure 1. *Cont.*

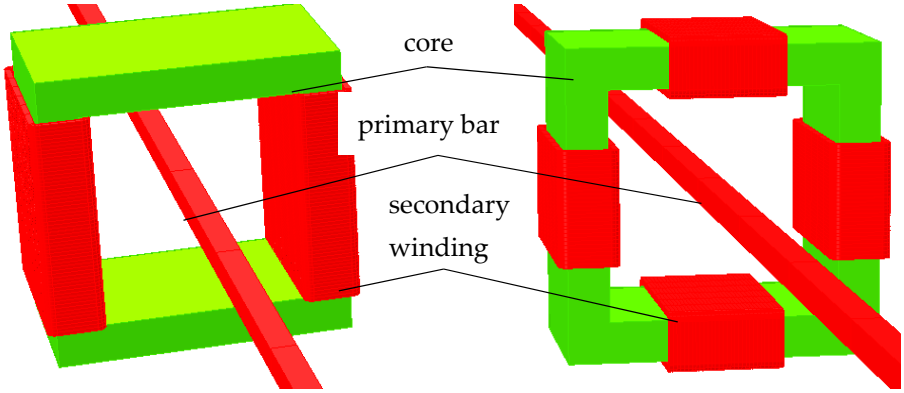

(**c**) split-core—model 2 (dimension: external a = 51.32 mm; internal b = 37.82 mm, height h = 30 mm).

(**d**) split-core—model 3 (dimension: external a = 51.32 mm; internal b = 37.82 mm, height h = 30 mm).

Figure 1. (**a**–**d**) 3D geometrical models of the measuring current transformers 600 A/5 A (number of turns = 120).

The toroidal current transformer's magnetic core was coiled from the strip made of cold-rolled steel sheets and formed one unit. Split-core current transformers have cores made of cold-rolled steel sheets, consisting of two parts to be disconnected. Figure 2 shows a 3D model of a split-core CT while mounted in a switchboard without disconnecting the bars.

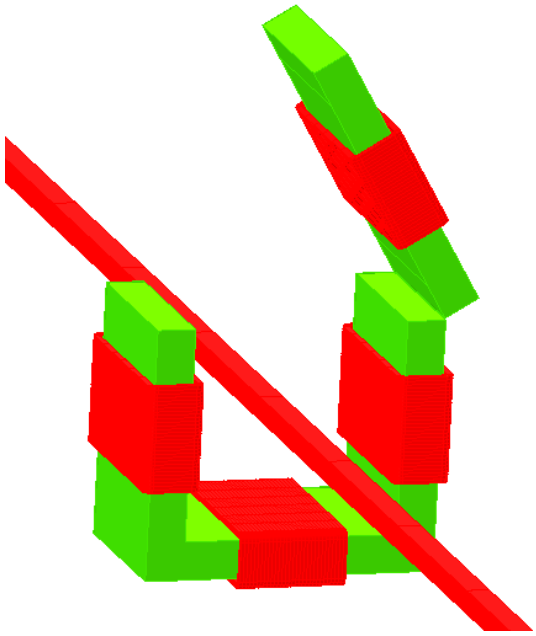

Figure 2. 3D geometrical model 3 of a split-core current transformer while mounted in a switchboard without disconnecting the bars.

Class S current transformers are intended for cooperation with measuring devices adapted to correctly measure the current in the range from 1% to 120% of the rated current (Table 1). This means that the metrologically defined range of secondary current for transformers with a rated secondary current of 5 A is from 50 mA to 6 A.

Problems with designing class S current transformers' magnetic circuits result from the necessity to use the magnetization characteristics and core material losses for extremely small values of magnetic flux density amplitude B_m. With currents of about 1% of the rated measurement current of a class S current transformer, the magnetic flux density amplitude

in the core is usually a few millitesla (mT), which requires knowledge of the core material characteristics at such a low level of magnetic induction.

The use of an inappropriate magnetization curve for computation leads to large discrepancies between the calculated and actual values of transformation errors. A linear approximation of the magnetic permeability and loss values distorts the results of the design calculations.

The ability to correctly determine the magnetization and core loss curves for the initial range of their course determines the correct calculation of transformer transformation errors, and the selection of the designed CT's electromagnetic circuit.

Manufacturers typically do not list initial magnetic material properties in their catalogs. Core manufacturers cannot guarantee that the magnetization and loss characteristics will be identical for each core in a given batch.

Therefore, CT designers should first measure the magnetic material's actual magnetic characteristics for the core [23–26].

The magnetization and loss characteristics of the transformer steel cores were performed for small-size ring samples ranging from a few milliteslas to the knee point induction, determined using the method described in the article [22]. Then, the Froelich method, which was repeatedly verified by various authors, [24,25] was used to extend the curve to the value of the saturation induction.

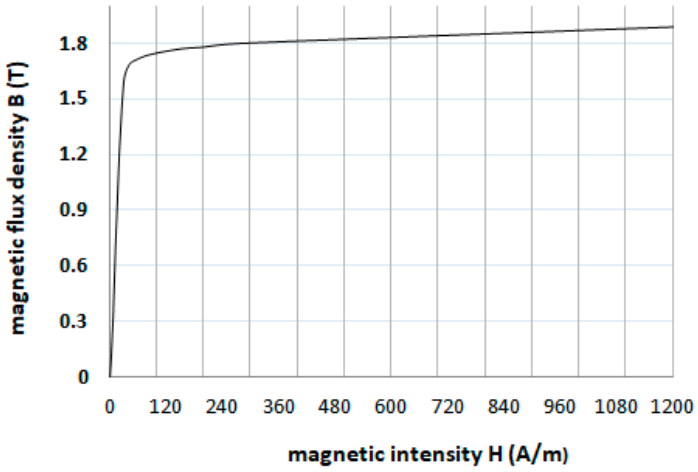

(**a**)

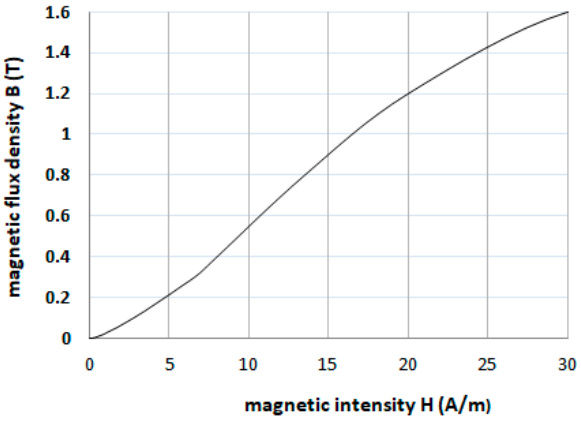

(**b**)

Figure 3. *Cont.*

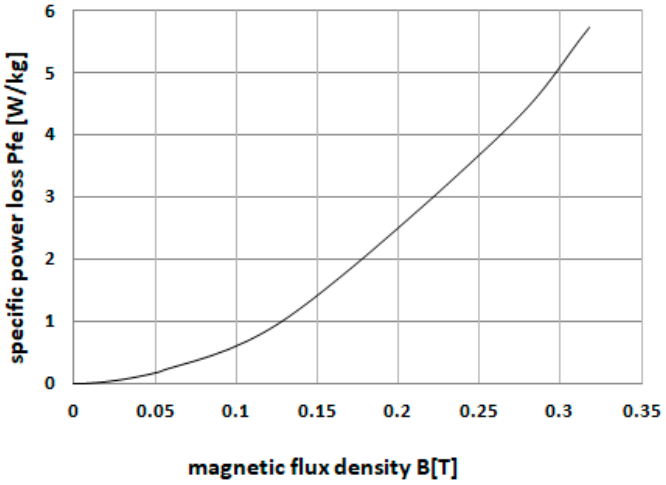

(**c**)

Figure 3. The measured magnetization characteristic of the magnetic materials used for the cores (**a**), its initial range (**b**) and specific power loss characteristics (**c**).

It is not always possible to measure the magnetization characteristics to very high currents in the laboratory, and manufacturers do not always provide the characteristics in saturation. On the other hand, computer programs during iteration also move along the characteristics in the saturation part. Therefore, a characteristic above the value at which the device operates is required. Froelich's mathematical method is based on the approximation of the magnetization characteristics by approximating the $1/\mu$ relationship with a linear function. For any value of H, we approximate $1/\mu$ with a linear function, next calculate μ, and then B. The assumption is that the dynamics of μ should be close to but less than 1. The accuracy of the approximation was defined by the coefficient of determination R^2.

3. Mathematical Model of CT

The problem of the accuracy of the operation of current transformers in the steady-state concerns sinusoidal alternating currents. The quasi-stationary electromagnetic field generated by these currents has a sine curve, i.e., harmonic field. This allows the use of complex numbers and the description of the electromagnetic field with the Helmholtz equation, resulting from the Maxwell equations, using the complex vector of the magnetic potential $\underline{\boldsymbol{A}}$ ($\underline{\boldsymbol{B}} = \nabla \times \underline{\boldsymbol{A}}$). As the standards [1,2] provide for testing transformation errors of current transformers at rated load, it is necessary to use the field-circuit method. This method consists of solving the field equations within the perimeter of the tested object in conjunction with the circuit's equation outside this area, i.e., the load connected to the current transformer's secondary terminals [13–19].

$$\nabla^2 \underline{\boldsymbol{A}} - \mu \nabla \left(\frac{1}{\mu} \right) \times \nabla \times \underline{\boldsymbol{A}} - j\omega\mu\sigma \underline{\boldsymbol{A}} = -\mu \underline{\boldsymbol{J}_w} \tag{3}$$

$$\underline{\Psi} = \frac{n_s}{S_s} \int_{\Omega_s} \underline{\boldsymbol{A}} \cdot \boldsymbol{l}_s dv \tag{4}$$

$$\underline{U_s} = j\omega \underline{\Psi} = (R + j\omega) \underline{I_s} \tag{5}$$

where R and L are the resistance and inductance of the burden of the secondary winding of the CT. ω is the angular frequency of the voltage. μ is the permeability. σ is the conductivity of the materials. $\underline{\psi}$ is the magnetic flux passing through the secondary coil. n_s and S_s are the number of turns and the cross-sectional area of this coil, respectively. Ω_s is the volume

of the secondary winding, and $\boldsymbol{l_s}$ is the unit tangential vector along the direction of the secondary current in the winding.

The boundary conditions for magnetic vector potential are $\underline{\boldsymbol{A}} \times \boldsymbol{n} = 0$, which means that at the boundary, only a tangential part of the magnetic flux density B appears, and $V = 0$ for electric scalar potential at the boundary of the entire system with the surrounding air.

The measured magnetization characteristic was used in field-circuit calculations. A method was also applied which took into account the power losses in laminated cores [20,22], based on the introduction of the core's hypothetical specific conductivity γ. This conductivity was calculated from the power lost in the real core.

The ELEKTRA STEADY-STATE module of the commercial software OPERA 3D (Version 19, Manufacturer 3DS, Paris, FRANCE) was used to calculate the magnetic field distribution and the secondary current. A division mesh of 9,415,326 elements was used for the 3D model.

The number of subdivision mesh elements was determined based on the accuracy analysis, when further mesh refinements did not change the solution and did not improve the accuracy.

4. Results of Computations and Tests

Transformation errors for all current transformer models were obtained by calculating the secondary currents using the field-circuit method and then using the definition formulas (1) and (2) given in the standards [1,2]. Figure 4 presents magnetic field distributions in the discussed cores of the current transformer models.

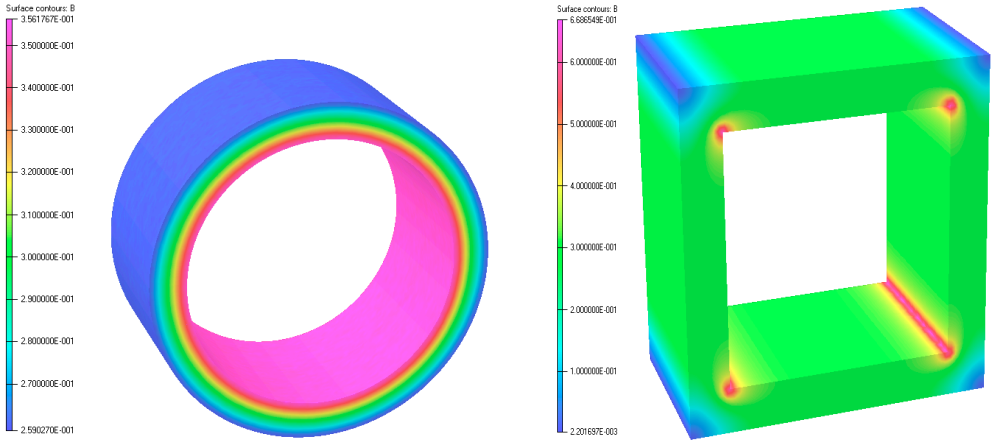

(**a**) (**b**)

Figure 4. Magnetic flux density distributions (T) of measuring current transformers 600 A/5 A at the rated primary current 600 A for two core versions (**a**) toroid core, (**b**) split -core.

The magnetic field distributions in all three models' rectangular cores are identical and differ only slightly in the maximum magnetic flux density value. On the other hand, the distribution of magnetic flux density in the rectangular and toroidal core differs significantly in Figure 4a,b.

The toroidal core physical model was tested with a comparator to measure the current error and phase displacement. The measurements were performed using a comparator manufactured by the OLTEST Company type CA507 (Table 2 provides information on the accuracy data of the CA507 comparator). Figure 5 shows the comparator used for transformation error measurements.

Table 2. The accuracy data of the CA507 comparator based on the user manual.

Secondary Current Range (A)	Range of the Permissible Values of the Absolute Uncertainty Δ_{FDI} (%)
from 1 to 7	$\pm(0.005 \cdot \lvert f_{DI} \rvert + 2 \times 10^{-4} + 0.03 \cdot \lvert \delta_{DI}/\delta_{DI\,max} \rvert)$
from 0.05 to 1	$\pm(0.005 \cdot \lvert f_{DI} \rvert + 3 \times 10^{-3} + 0.03 \cdot \lvert \delta_{DI}/\delta_{DI\,max} \rvert)$
from 0.01 to 0.05	$\pm(0.005 \cdot \lvert f_{DI} \rvert + 1.5 \times 10^{-2} + 0.03 \cdot \lvert \delta_{DI}/\delta_{DI\,max} \rvert)$
Secondary current range (A)	**Range of the permissible values of the absolute uncertainty $\Delta\delta_{DI}$ (min)**
from 0.25 to 7	$\pm(0.005 \cdot \lvert \delta_{DI} \rvert + 0.03 + 0.7 \cdot \lvert f_{DI}/f_{DI\,max} \rvert)$
from 0.01 to 0.25	$\pm(0.005 \cdot \lvert \delta_{DI} \rvert + 0.5 + 0.7 \cdot \lvert f_{DI}/f_{DI\,max} \rvert)$

where: f_{DI}—measurement result of the relative difference of the secondary currents of two CTs, expressed in percentages; δ_{DI}—measurement result of the phase difference of the secondary currents of two CTs, expressed in minutes; $f_{DI\,max}$—upper limit value of the measuring range for the relative difference of secondary currents of two CTs, equal to 15%; $\delta_{DI\,max}$—the upper limit value of the measurement range for the phase difference of the secondary currents of two CTs, equal to 300 min.

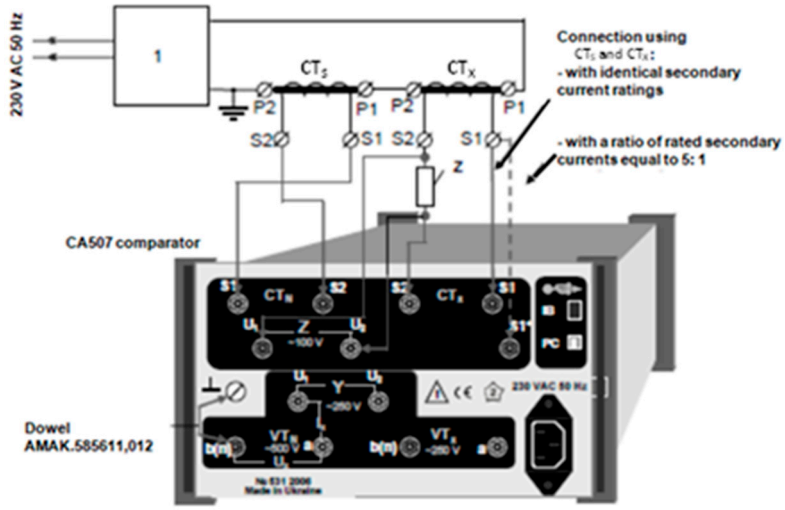

(**a**)

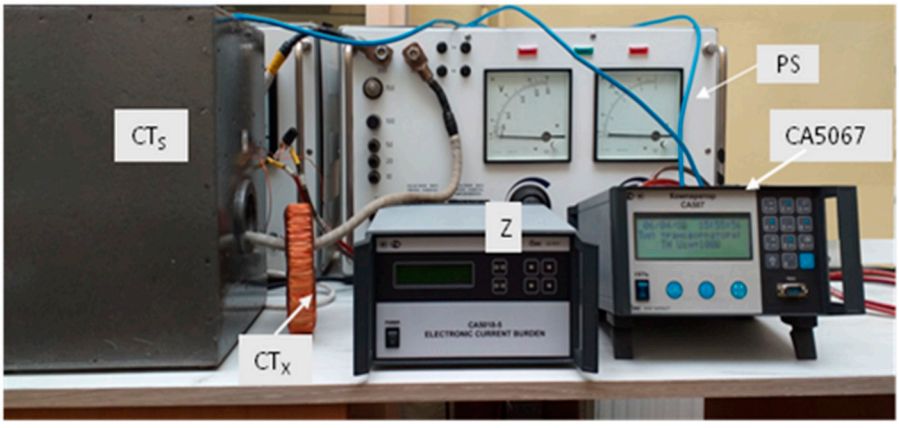

(**b**)

Figure 5. (**a**) Diagram and (**b**) picture of the system for measuring transformation errors of current transformers: CA507 = comparator; PS = power supply system—current source, consisting of a voltage regulator and a transformer; CT_S = reference current transformer; CT_X = tested current transformer; Z = impedance—secondary winding burden of the tested transformer.

The characteristics of the current error and phase displacement error, obtained from the calculations and measurements of the 600 A/5 A current transformer with a toroidal core,

were compared under the same conditions. Figures 6 and 7 show a comparison of calculated and measured transformation errors of the tested CT (Figure 8) at different burdens.

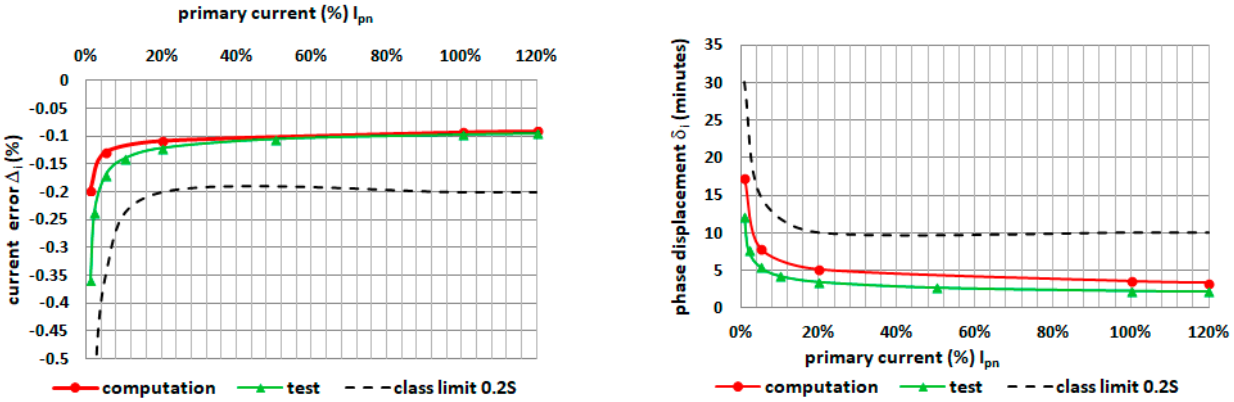

(**a**) current errors (**b**) phase displacement

Figure 6. Comparison of the characteristics of the current error (**a**) and phase displacement (**b**) from the calculations and tests for 600 A/5 A current transformers with a toroidal core at a power load of S_n = 2.5 VA. cosϕ = 0.8 (I_{pn} = 600 A).

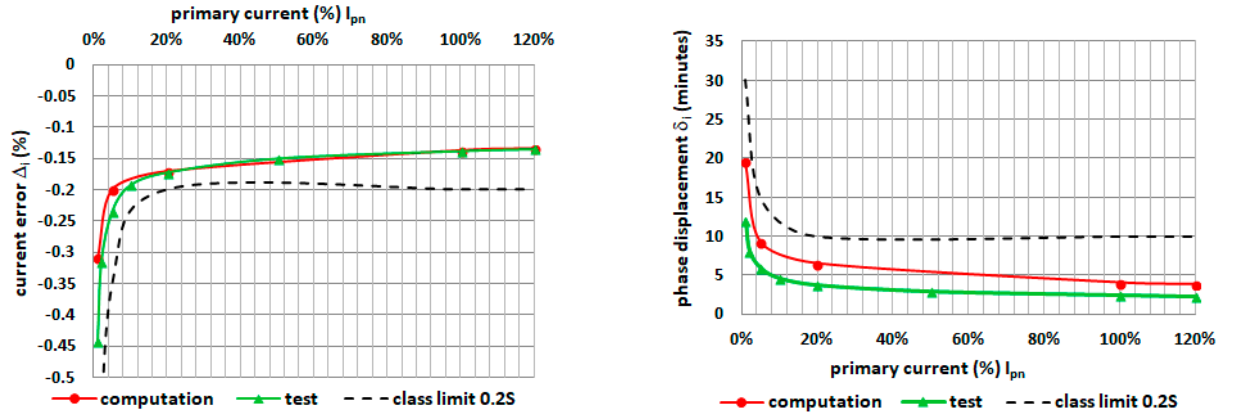

(**a**) current errors (**b**) phase displacement

Figure 7. Comparison of the characteristics of the current error (**a**) and phase displacement (**b**) from the calculations and tests for 600 A/5 A current transformers with a toroidal core at a power load of S_n = 5 VA. cosϕ = 0.8 (I_{pn} = 600 A).

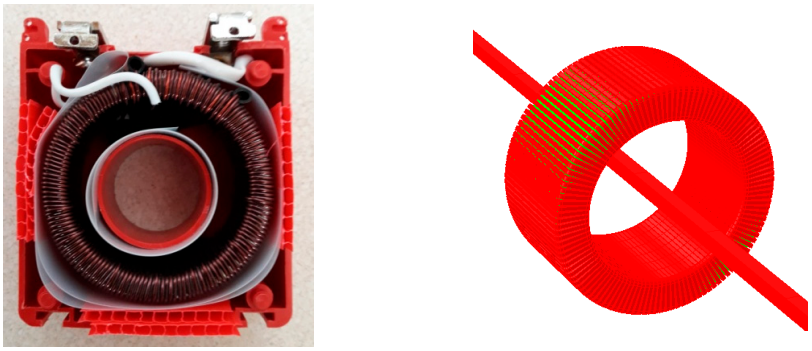

(**a**) (**b**)

Figure 8. Toroidal current transformer type ELA 600 A/5 A class 0.2S (**a**) and its numerical model (**b**).

Comparing the calculated and measured transformation errors of the tested current transformer with the toroidal core gave similar results, which confirms the accuracy of the applied field-circuit method.

The transformation accuracy of various current transformer models was tested under the following conditions (compliant with the [1,2] standards): the primary winding was supplied with a primary current of a different percentage of the rated current (600 A), and the secondary winding was loaded with an impedance of 5 VA and cosφ = 0.8 as well as 2.5 VA and cosφ = 0.8.

The characteristics of the current error and phase displacement of four models of the 600 A/5 A current transformer with different cores and secondary winding arrangements were compared under the same conditions. Figures 9 and 10 show the transformation errors for all four tested current transformer models.

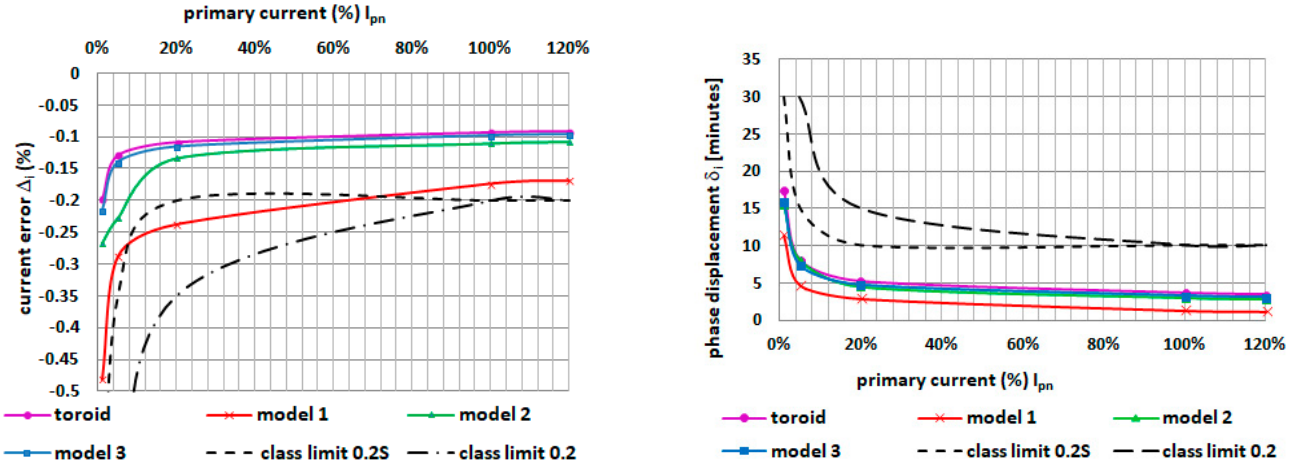

(**a**) current errors (**b**) phase displacement

Figure 9. Comparison of the characteristics of the current error (**a**) and phase displacement (**b**) for 600 A/5 A of current transformers with different cores and secondary windings arrangements at a power load of S_n = 2.5 VA. cosϕ = 0.8 (I_{pn} = 600 A) S_n = 2.5 VA. cosϕ = 0.8 (I_{pn} = 600 A).

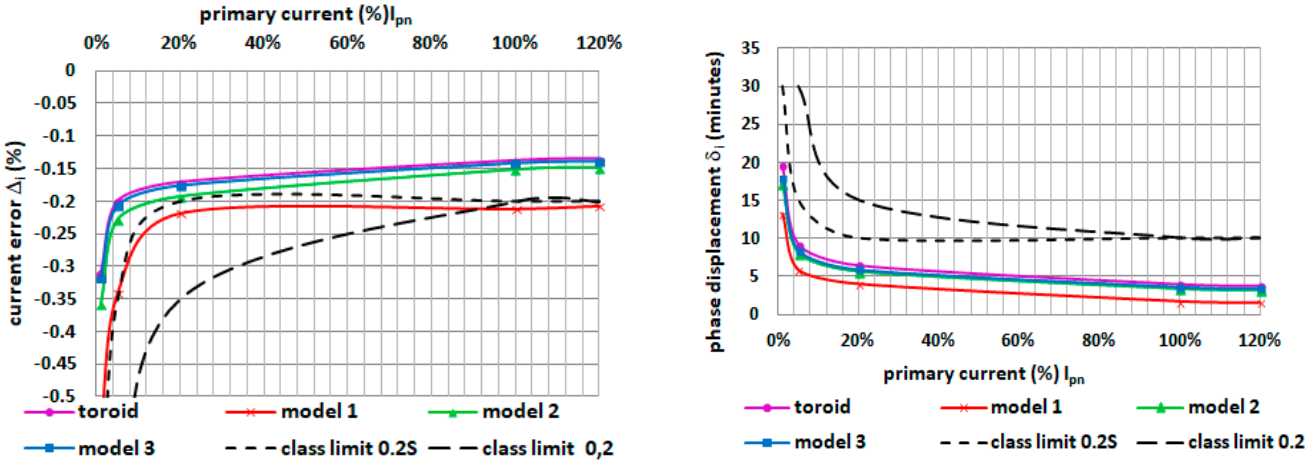

(**a**) current errors (**b**) phase displacement

Figure 10. Comparison of the characteristics of the current error (**a**) and phase displacement (**b**) for 600 A/5 A of current transformers with different cores and secondary windings arrangements at a power load of S_n = 5 VA. cosφ = 0.8 (I_{pn} = 600 A).

The analysis results show that the arrangement of the secondary windings on rectangular split-cores impacts current measurement accuracy with this type of transformer. Unfortunately, it is impossible to arrange the secondary winding evenly on such cores as on a toroidal core. Even more so, it is not possible to divide the toroidal cores.

Model 1 of the current transformer with windings wound in two layers on one column is the simplest to build (Figure 11). On the other hand, with the same load and power supply conditions, it has the lowest measurement accuracy of current among all the considered models. The characteristics of its current errors exceed the permissible limits of not only the 0.2S class but also the 0.2 class, both when loaded with rated power S_n = 2.5 VA and 5 VA. With this accuracy, a current transformer is class 0.5, regardless of the load with the rated power of 2.5 VA or 5 VA.

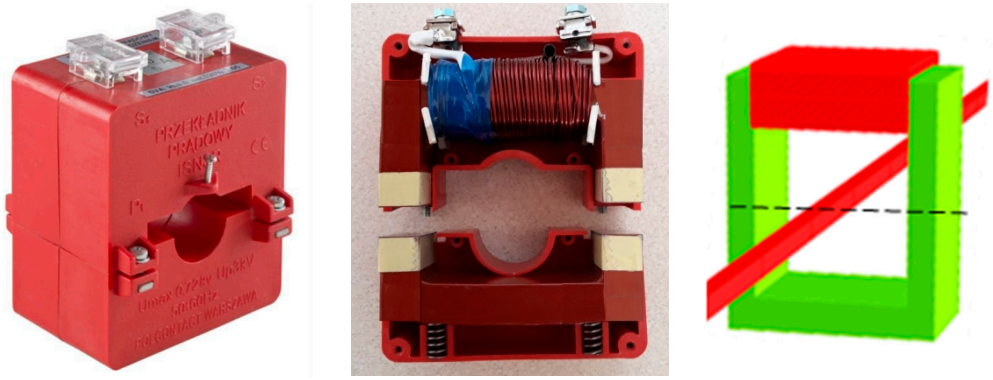

(**a**) (**b**) (**c**)

Figure 11. Split-core current transformer type ISN 3R 600 A/5 A class 0.5: in the housing (**a**), interior (**b**), and its numerical Model 1 (**c**).

The Model 2 CT has a split secondary winding, wound in one layer, distributed over two columns, and connected in series. Such a model is more difficult to make but may have a split-core. (Figure 12)

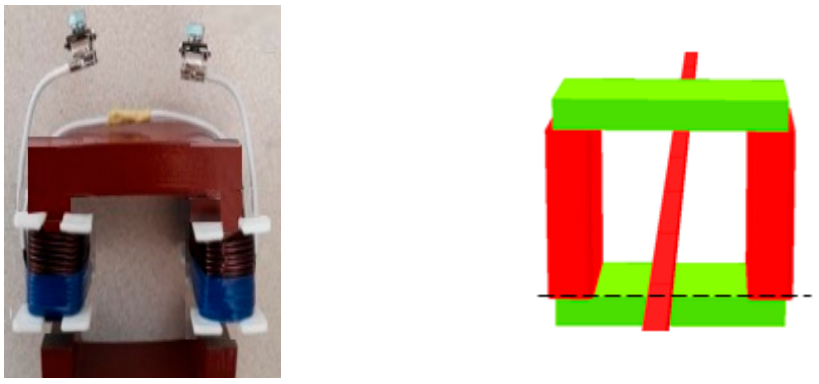

(**a**) (**b**)

Figure 12. Prototype split-core current transformer of (**a**) Model 2 class 0.2S: and (**b**) its numerical model.

The Model 3 CT has a secondary winding split into four parts, wound in one layer, connected in series, and distributed over the four parts of the core. The accuracy of Model 2 also meets the 0.2S criteria, and its design is easier to manufacture and can therefore be recommended for use in practice.

Model 3 achieves the best accuracy, not least because both the current error characteristics and the phase displacement meet the conditions of class 0.2S at various rated

power loads, but also almost achieve the accuracy of a current transformer with an evenly distributed winding on the toroidal core. Both of these current transformers' accuracy under a load of 2.5 VA is close to class 0.1. They slightly exceed the limit of class 0.1 with a primary current of 20% of the rated current. The obtained results indicate that voltage errors and phase displacement values are appropriate for the accuracy class 0.2S.

Both Models 2 and 3 of the current transformers meet the accuracy class of 0.2S with a rated load of S_n = 2.5 VA and 5 VA.

5. Conclusions

This article presents research results on such a split-core current transformer structure that will ensure the high accuracy of this device during measurements (according to the standards [1,2]).

Research conducted with numerical methods and physical tests on the same transformer's real model gave convergent results. The accuracy of the field-circuit method used has been confirmed. Constructors using the 3D field-circuit-method simulation method can accurately predict the magnetic field distribution and transformation errors of different transformer designs of current transformers. The computation and test results show this.

The application of split-cores with a specific design allows for a higher accuracy class of this type of current transformer. As a result of the conducted research, the highest accuracy transformer construction model was selected. Model 3 is the current transformer model that gives the certainty of obtaining the best accuracy, similar to that of a non-demountable current transformer, i.e., with a toroidal core.

Model 3 is also the most time-consuming to perform. The accuracy of Model 2 also meets the 0.2S criteria, and its design is easier to manufacture and can, therefore, be recommended for use in practice.

The use of 3D modeling to test the accuracy of spit-core current transformers is an aspect that has not yet been addressed in the literature.

Failure to comply with the standards regarding the accuracy of measuring split-core current transformers results in an increase in the measuring systems' errors during assembly, in distribution panels in places where it is impossible to install classic current transformers.

Funding: This research received no external funding.

Institutional Review Board Statement: Not applicable.

Informed Consent Statement: Not applicable.

Data Availability Statement: The data presented in this study are available on request from the corresponding author. Computer data are not publicly available because they are not suitable for use by other researchers.

Acknowledgments: I would like to thank the producers of POLCONTACT Warszawa for inspiration for research on the accuracy of various solutions for split-core current transformers, as well as for the implementation and availability for tests of the toroidal current transformer, the current transformer with a split-core and winding on one column (Model 1) and the prototype of Model 2.

Conflicts of Interest: The author declares no conflict of interest.

References

1. *IEC/EN 61869-1. Instrument Transformers-Part 1: General Requirements*; International Electrotechnical Commission: Geneva, Switzerland, 2009.
2. *IEC/EN 61869-2. Instrument Transformers-Part 2: Additional Requirements for Current Transformer*; International Electrotechnical Commission: Geneva. Switzerland, 2012.
3. Suarez, A.; Victoria, J.; Torres, J.; Martinez, P.A.; Alcarria, A.; Perez, J.; Garcia-Olcina, R.; Soret, J.; Muetsch, S.; Gerfer, A. Performance Study of Split Ferrite Cores Designed for EMI Suppression on Cables. *Electronics* **2020**, *9*, 1992. [CrossRef]
4. Bhuiyan, R.H.; Dougal, R.A.; Ali, M. A Miniature Energy Harvesting Device for Wireless Sensors in Electric Power System. *IEEE Sens. J.* **2010**, *10*, 1249–1258. [CrossRef]

5. Lim, T.; Kim, Y. Compact Self-Powered Wireless Sensors for Real-Time Monitoring of Power Lines. *J. Electr. Eng. Technol.* **2019**, *14*, 1321–1326. [CrossRef]
6. Lopes, I.; Valle, R.; Fogli, G.; Ferreira, A. Low-Frequency Underwater Wireless Power Transfer: Maximum Efficiency Tracking Strategy. *IEEE Latin Am. Trans.* **2020**, *18*, 1200–1208. [CrossRef]
7. Miron-Alexe, V. Comparative Study Regarding Measurements of Different AC Current Sensors. In Proceedings of the International Symposium on Fundamentals of Electrical Engineering (ISFEE), Bucharest, Romania, 30 June–2 July 2016. [CrossRef]
8. Das, J.C.; Multikin, R. Design and Application of a Low-Ratio High-Accuracy Split-Core Core-Balance Current Transformer. *IEEE Trans. Ind. Appl.* **2010**, *46*, 1856–1865. [CrossRef]
9. Doig, P.; Gunn, C.; Durante, L.; Burns, C.; Cochrane, M. Reclassification of relay-class current transformers for revenue metering applications. In Proceedings of the IEEE/PES Transmission & Distribution Conference & Exposition, Dallas, TX, USA, 21–24 May 2006. [CrossRef]
10. Dems, M.; Komeza, K.; Lecointe, J.P. Influence of massive ferromagnetic shaft on the distribution of electromagnetic field and magnetising current for two- and four-pole induction motors at frequencies of 50 and 200 Hz. *IET Electr. Power Appl.* **2018**, *12*, 1407–1416. [CrossRef]
11. Witczak, P.; Swiatkowski, M. Magnetic forces applied to the tank walls of a large power transformer. *COMPEL-Int. J. Comput. Math. Electr. Electron. Eng.* **2016**, *35*, 2087–2094. [CrossRef]
12. Amoiralis, E.I.; Georgilakis, P.S.; Tsili, M.A.; Kladas, A.G. Global transformer optimization method using evolutionary design and numerical field computation. *IEEE Trans. Magn.* **2009**, *45*, 1720–1723. [CrossRef]
13. Milenov, I.; Yatchev, I. CAD System-Boundary Integral Equation Method for 3D Electric Field Analysis of Voltage Transformers. In *Transformers, Analysis, Design and Measurement*; Lopez-Fernandez, X.M., Ertan, B.H., Turowski, J., Eds.; CRC Press Taylor & Francis Group: Boca Raton, FL, USA; London, UK; New York, NY, USA, 2012; pp. 381–397.
14. Kumbhar, G.B.; Mahajan, S.M. Analysis of short circuit and inrush transients in a current transformer using a field-circuit coupled FE formulation. *Int. J. Electr. Power Energy Syst.* **2011**, *33*, 1361–1367. [CrossRef]
15. Lesniewska, E. Applications of the Field Analysis during Design Process of Instrument Transformers. In *Transformers, Analysis, Design and Measurement*; Lopez-Fernandez, X.M., Ertan, B.H., Turowski, J., Eds.; CRC Press Taylor & Francis Group: Boca Raton, FL, USA; London, UK; New York, NY, USA, 2012; pp. 349–380.
16. Lesniewska, E.; Jalmuzny, W. The estimation of metrological characteristics of instrument transformers in rated and overcurrent conditions based on the analysis of electromagnetic field. *Int. J. Comput. Math. Electr. Electron. Eng.* **1992**, *11*, 209–912. [CrossRef]
17. Lesniewska, E.; Chojnacki, J. Influence of the Correlated Localisation of Cores and Windings on Measurement Properties of Current Transformers. *Electromagn. Fields Electr. Eng.* **2002**, *22*, 236–241.
18. Lesniewska, E.; Rajchert, R. Influence of different load of the secondary winding on measurement properties of current transformers with core made from different magnetic materials. *IET Sci. Meas. Technol.* **2019**, *13*, 944–948. [CrossRef]
19. Lesniewska, E.; Lisowiec, A. Estimation of Influence of External Magnetic Field on New Technology Current-to-Voltage Transducers Operating in Protection System of AC Power Networks. *IEEE Trans. Power Deliv.* **2016**, *31*, 541–550. [CrossRef]
20. IEC/EN 61869-7. *Instrument Transformers-Part 8: Additional Requirements for Electronic Current Transformers*; International Electrotechnical Commission: Geneva, Switzerland, 2012.
21. Kaczmarek, M.; Kaczmarek, P. Comparison of the Wideband Power Sources Used to Supply Step-Up Current Transformers for Generation of Distorted Currents. *Energies* **2020**, *13*, 1849. [CrossRef]
22. Lesniewska, E.; Kaczmarek, M.; Stano, E. 3D Electromagnetic Field Analysis Applied to Evaluate the Accuracy of a Voltage Transformer under Distorted Voltage. *Energies* **2021**, *14*, 136. [CrossRef]
23. Markovic., M.; Perriard., Y. Eddy current power losses in a toroidal laminated core with rectangular cross section. In Proceedings of the 12th International Conference on Electrical Machines and Systems, Tokyo, Japan, 15–18 November 2009; pp. 1–4. [CrossRef]
24. Diez, P.; Webb, J.P. A Rational Approach to B-H Curve Representation. *IEEE Trans. Magn.* **2016**, *52*, 1–4. [CrossRef]
25. Trutt, F.C.; Erdelyi, E.A.; Hopkins, R.E. Representation of the Magnetization Characteristic of DC Machines for Computer Use. *IEEE Trans. Power Appar. Syst.* **1968**, *87*, 665–669. [CrossRef]
26. Kefalas, T.D.; Georgilakis, P.S.; Kladas, A.G.; Souflaris, A.T.; Paparigas, D.G. Multiple Grade Lamination Wound Core a Novel Technique forTransformer Iron Loss Minimization Using Simulated Annealing with Restarts and an Anisotropy Model. *IEEE Trans. Magn.* **2008**, *44*, 1082–1085. [CrossRef]